

IEEE

GEOSCIENCE AND REMOTE SENSING LETTERS

A PUBLICATION OF THE IEEE GEOSCIENCE AND REMOTE SENSING SOCIETY



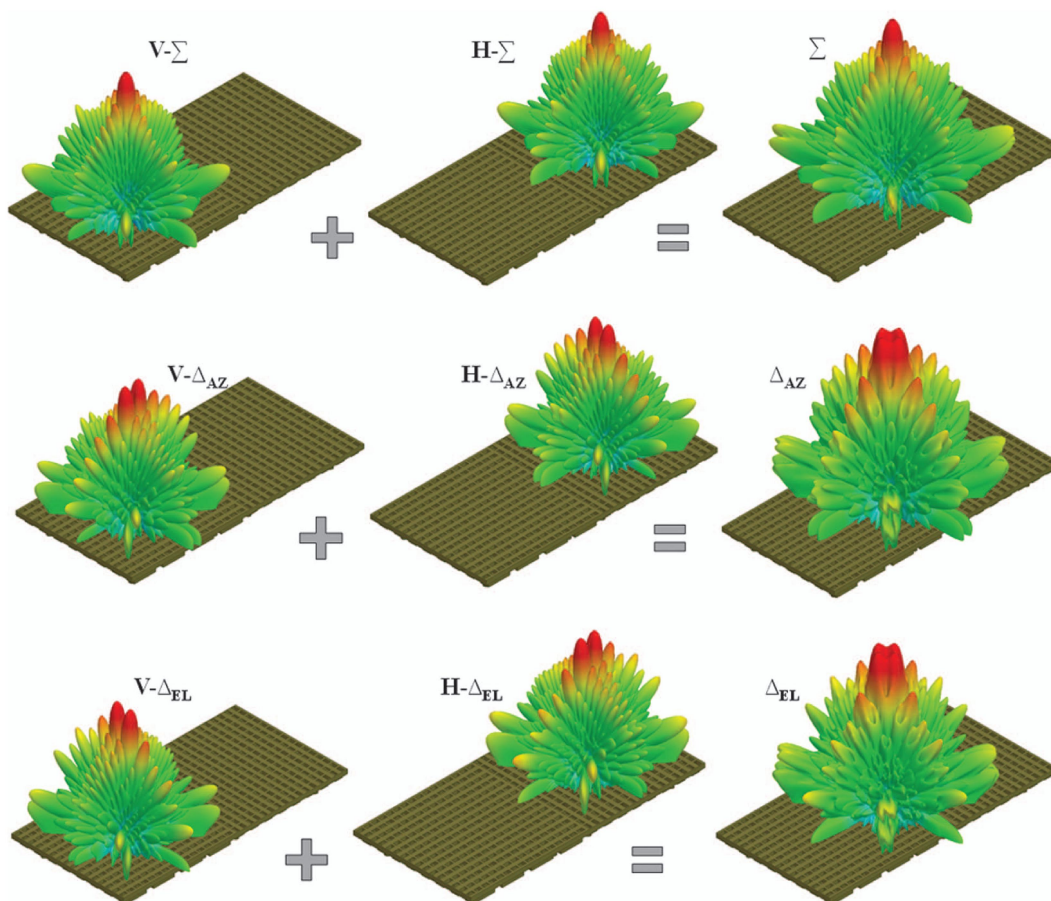
AUGUST 2016

VOLUME 13

NUMBER 8

IGRSBY

(ISSN 1545-598X)



Synthesis of array radiation patterns for different monopulse scenarios.

IEEE

GEOSCIENCE AND REMOTE SENSING LETTERS

A PUBLICATION OF THE IEEE GEOSCIENCE AND REMOTE SENSING SOCIETY



AUGUST 2016

VOLUME 13

NUMBER 8

IGRSBY

(ISSN 1545-598X)

PAPERS

Oceans and Water

Image Analysis for Altimetry Waveform Selection Over Heterogeneous Inland Waters *A. Marshall and X. Deng* 1198

Cryosphere

Uniaxial Effective Permittivity of Anisotropic Bicontinuous Random Media Using NMM3D
. *S. Tan, C. Xiong, X. Xu, and L. Tsang* 1168

Vegetation and Land Surface

A Study of Land Surface Albedo Conversion Formulas Using Three-Dimensional Canopy Radiative Transfer Modeling
. *J. Adams, N. Gobron, and C. Mio* 1039

Surface and Subsurface Properties

Improved Envisat Altimetry Ice Sheet Elevation Change Data Processing Algorithms Using Repeat-Track Analysis . . .
. *X. Su, C.-K. Shum, C. Kuo, and Y. Yi* 1099

SNR Enhancement for Downhole Microseismic Data Using CSST *H. Zhao, Y. Li, and C. Zhang* 1139

An Improvement on SSA Method for EM Scattering From Electrically Large Rough Sea Surface
. *J. Li, M. Zhang, P. Wei, and W. Jiang* 1144

Image Processing, Analysis, and Classification

An Adaptive Filter for Aeromagnetic Compensation Based on Wavelet Multiresolution Analysis
. *Z. Dou, Q. Han, X. Niu, X. Peng, and H. Guo* 1069

Ship Rotated Bounding Box Space for Ship Extraction From High-Resolution Optical Satellite Images With Complex
Backgrounds *Z. Liu, H. Wang, L. Weng, and Y. Yang* 1074

Efficient Airport Detection Using Line Segment Detector and Fisher Vector Representation
. *Ü. Budak, U. Halıcı, A. Şengür, M. Karabatak, and Y. Xiao* 1079

Simulated Annealing With Variogram-Based Optimization to Quantify Spatial Patterns of Trees Extracted From
High-Resolution Images *V. Srivastava, A. Stein, D. G. Rossiter, P. K. Garg, and R. D. Garg* 1084

An Elaborately Designed Virtual Frame to Level Aeromagnetic Data *Z. Fan, L. Huang, X. Zhang, and G. Fang* 1153

Change Detection Using Global and Local Multifractal Description
. *S. Aleksandrowicz, A. Wawrzaszek, W. Drzewiecki, and M. Krupiński* 1183

Disaster Damage Assessment of Buildings Using Adaptive Self-Similarity Descriptor
. *F. Kahraman, M. Imamoglu, and H. F. Ates* 1188

(Contents Continued on Page 1038)



| | |
|---|------|
| Hyperspectral Data Processing | |
| A Modified Locality-Preserving Projection Approach for Hyperspectral Image Classification | 1059 |
| Y. Zhai, L. Zhang, N. Wang, Y. Guo, Y. Cen, T. Wu, and Q. Tong | |
| A Target Detection Method Based on Low-Rank Regularized Least Squares Model for Hyperspectral Images | 1129 |
| Y. Xu, Z. Wu, F. Xiao, T. Zhan, and Z. Wei | |
| Radar Systems | |
| Three-Dimensional Electromagnetic Model-Based Pose Estimation Using Fully Polarimetric Wideband Radar | 1054 |
| X. Yang, G. Wen, C. Ma, S. Qiu, and B. Ding | |
| An Improved Oblique Projection Method for Sea Clutter Suppression in Shipborne HFSWR | 1089 |
| C. Yi, Z. Ji, T. Kirubarajan, J. Xie, and B. Hu | |
| Attenuation of Millimeter-Wave in a Sand and Dust Storm | 1094 |
| M.-M. Chiou and J.-F. Kiang | |
| The Stability of UWB Low-Frequency SAR Images | 1114 |
| R. Machado, V. T. Vu, M. I. Pettersson, P. Dammert, and H. Hellsten | |
| ASCAT and QuikSCAT Azimuth Modulation of Backscatter Over East Antarctica | 1134 |
| R. D. Lindsley and D. G. Long | |
| Polarimetric Calibration Based on Lexicographic-Basis Decomposition | 1149 |
| J. Lin, Y. Guo, W. Li, Y. Zhang, and Z. Chen | |
| Attitude-Steering Strategy for Squint Spaceborne Synthetic Aperture Radar | 1163 |
| S. Zhao, Y. Deng, and R. Wang | |
| Side-Lobe Reduction for Radio Frequency Interference Suppression via Clipping of Strong Scatterers | 1178 |
| Y.-L. Li, X.-Y. Li, and Z.-M. Zhou | |
| Microwave Radiometry | |
| Bayesian Inference for Inversion in Synthetic Aperture Imaging Radiometry | 1049 |
| L. Wu, F. Hu, F. He, and J. Li | |
| On the Spatial Resolution of GNSS Reflectometry | 1064 |
| M. P. Clarizia and C. S. Ruf | |
| Results of Real-Time Kinematic Positioning Based on Real GPS L5 Data | 1193 |
| X. Luo, S. Li, and H. Xu | |
| Synthetic Aperture Radar | |
| Improved Multiscale Edge Detection Method for Polarimetric SAR Images | 1104 |
| R. Jin, J. Yin, W. Zhou, and J. Yang | |
| Range-Cell-Focusing Algorithm Combined With Enhanced MUSIC for Close Target Imaging | 1109 |
| Y.-S. Cho, H.-K. Jung, C. Cheon, J. So, and Y.-S. Chung | |
| Experimental Results of Passive SAR Imaging Using DVB-T Illuminators of Opportunity | 1124 |
| D. Gromek, K. Kulpa, and P. Samczyński | |
| Range-Dependent Map-Drift Algorithm for Focusing UAV SAR Imagery | 1158 |
| L. Zhang, M. Hu, G. Wang, and H. Wang | |
| Lidar Systems | |
| Anisotropy Characteristics of Exposed Gravel Beds Revealed in High-Point-Density Airborne Laser Scanning Data | 1044 |
| G.-H. Huang, C.-K. Wang, F.-C. Wu, and P. M. Atkinson | |
| Junction-Based Correspondence Estimation of Plant Point Cloud Data Using Subgraph Matching | 1119 |
| A. Chaudhury, M. Brophy, and J. L. Barron | |
| AP SAR 2015 | |
| Onboard Processing for Data Volume Reduction in High-Resolution Wide-Swath SAR | 1173 |
| M. Villano, G. Krieger, and A. Moreira | |
| Wideband Dual-Polarized and Dual-Monopulse Compact Array for SAR System Integration Applications | 1203 |
| G.-L. Huang, S.-G. Zhou, T.-H. Chio, C.-Y.-D. Sim, and T.-S. Yeo | |

ANNOUNCEMENTS

| | |
|--|------|
| Call for Papers—IEEE JOURNAL OF SELECTED TOPICS IN APPLIED EARTH OBSERVATIONS AND REMOTE SENSING Special Issue on the 2016 IGARSS Symposium | 1208 |
|--|------|

About the Cover: A wideband dual-polarized and dual-monopulse array has been developed for SAR system integration applications. This figure demonstrates the synthesis procedures of array radiation patterns for different monopulse scenarios. Different patterns can be generated by different combination of ports' excitation. When the Σ ports of horizontal and vertical polarizations are excited simultaneously, only a mainbeam will be generated in the broadside direction. While the Δ_{AZ} ports of the two polarizations are excited, a unique pattern of four-beam with a null at the center can be obtained. The pattern generation principle of the Δ_{EL} ports is the same as the Δ_{AZ} ones. For more information please see "Wideband Dual-Polarized and Dual-Monopulse Compact Array for SAR System Integration Applications" by Huang *et al.*, which begins on page 1203.